THE EFFECT OF ION DRIFTS ON THE PROPERTIES OF THE TOKAMAK SCRAPE-OFF PLASMA

PPPL--2554

DE89 001176

M. Petravic and G. Kuo-Petravic

Plasma Physics Laboratory, Princeton University

Princeton, NJ 08543

ABSTRACT

A plasma fluid model which takes into account ion drifts has been constructed and applied to the scrape-off layer of a tokamak with a poloidal divertor. This model predicts near-sonic toroidal velocities and large poloidal flows in most of the scrapeoff together with steep gradients in the pressure and electrostatic potential along the magnetic field near the X-point, contrary to the predictions of the standard model. The potential step at X-point should reduce parallel heat transport and could act as an H-mode trigger.

The properties of scrape-off plasmas in the tokamaks with poloidal divertors have been studied for a number of years by solving numerically fluid models with sources arising from plasma-neutral gas interaction. A number of 2-D codes have been developed[1-6] based on the Braginskii equations[7] or their equivalent. The so-called high recycling regime[8] has been studied in detail. The most important findings have been the lowering of the plasma temperature to ≈ 10 eV in the recycling region, and the confinement of the recycling neutral gas to a volume close to the neutralizer plate. The properties of these solutions have been described in detail,[9] the most important characteristics being a highly subsonic flow and constant plasma pressure along the magnetic field lines everywhere except in the recycling region where the plasma is accelerated to the speed of sound, and the plasma pressure drops by a factor of two. Despite the fact that poloidal divertors have been instrumental in producing the H-mode confinement,[10] no plasma feature has been found in these solutions that might distinguish a divertor from a limiter plasma. This paper shows that when ion drifts due to electric fields and pressure gradients are taken into account, the plasma solution outside the recycling (plate) region changes dramatically; the toroidal velocities become near-sonic, substantial poloidal flows develop around the main plasma, and large pressure and potential steps arise near the X-point. These features depend nonlinearly on temperature, and their magnitude is a function of both the magnitude and orientation of the magnetic field. Combining these findings with the expected reduction of the parallel electron heat conduction caused by the potential steps, a plausible model for an H-mode trigger can be constructed.

Singer and Langer[11] have derived a set of fluid equations valid under highly subsonic conditions, which explicitly include the ion-drift terms due

to both the electric fields and the ion pressure gradients. We have here assumed that the Braginskii equations are valid in the trans-sonic regime, and have derived a set of fluid equations (1)-(4) which differ from those of Singer and Langer in that the $\nabla_{\parallel} p$ term in the potential [Eq. (3)] and the parallel viscosity have been retained and $T_e = T_i$ has been assumed. In deriving these equations, two coordinate systems have been used: a system defined by the unit vectors $\underset{\sim}{b} = \underset{\sim}{B}/|\underset{\sim}{B}|$, $\nabla\psi \times \underset{\sim}{b}/|\nabla\psi \times \underset{\sim}{b}|$, and $\nabla\psi/|\nabla\psi|$, with the corresponding spatial variables (ξ,ζ,ψ), where ψ is the poloidal magnetic flux, and the (ϕ,θ,ψ) system, where ϕ and θ are the toroidal and poloidal angles, respectively. The relationship between the two systems is shown in Fig. 1. The Eqs. (1)-(4) are steady-state Braginskii equations in conservative form representing particle (ion) conservation, ion momentum conservation, force balance for electrons, and the total energy conservation, respectively.

$$\nabla_{\parallel}\left(nv_{\theta}\frac{B}{B_{\theta}}\right) = S_n - \nabla_{\psi}\left(nv_{\psi}\right) \quad , \tag{1}$$

$$\nabla_{\parallel}\left(mnv_{\parallel}v_{\theta}\frac{B}{B_{\theta}}\right) = -\underset{\sim}{\nabla}_{\parallel}(2nT) + S_p - \nabla_{\psi}\left(mnv_{\parallel}v_{\psi}\right) + \nabla_{\parallel}\left(\eta_o \underset{\sim}{\nabla}_{\parallel} v_{\parallel}\right)$$

$$+ \frac{B_{\phi}}{B_{\theta}}\nabla_{\parallel}\left(\eta_4 \underset{\sim}{\nabla}_{\psi} v_{\parallel}\right) + \nabla_{\psi}\left(\eta_4 \frac{B_{\phi}}{B_{\theta}} \underset{\sim}{\nabla}_{\parallel} v_{\parallel}\right) \quad , \tag{2}$$

$$e\underset{\sim}{\nabla}_{\parallel}\phi = \frac{1}{n}\underset{\sim}{\nabla}_{\parallel}(nT) + 0.71\,\underset{\sim}{\nabla}_{\parallel}T \quad , \tag{3}$$

$$\nabla_{\parallel}\left[\left(\frac{5}{2}T + \frac{m}{2}v_{\parallel}^2\right) nv_{\theta}\frac{B}{B_{\theta}} - \chi_{\parallel}\underset{\sim}{\nabla}T\right]$$

$$= S_E - \nabla_{\psi}\left[\left(\frac{5}{2}T + \frac{m}{2}v_{\parallel}^2\right) nv_{\psi} - \chi_{\psi}\underset{\sim}{\nabla}_{\psi}T\right] + \frac{4}{3}\eta_o\left(\underset{\sim}{\nabla}_{\parallel}v_{\parallel}\right)^2 \quad . \tag{4}$$

Here $n = n_e = n_i$ and $T = T_e = T_i$ are the plasma density and temperature; $v_\parallel$, v_ψ, and v_θ are the parallel, radial, and poloidal ion velocity, respectively; and m is the ion mass. B_ψ and B_θ are the toroidal and poloidal magnetic field components, $B = (B_\phi^2 + B_\theta^2)^{1/2}$, and Φ is the electrostatic potential. S_n, S_p, and S_E are the particle (ion), momentum and energy sources arising from the ionization of neutrals, $\chi_\parallel$ and χ_ψ are the parallel and radial heat conductivities, and $\eta_0 = nT\tau$ and $\eta_4 = \eta_0(\omega\tau)^{-1}$ are the classical viscosity coefficients. (ω is the ion gyro-frequency and τ is the ion collision time.) Viscous terms of the order $\eta_0(\omega\tau)^{-2}$ have been neglected. In our model only charge neutrality and parallel force balance are used for electrons, which amounts to neglecting the effect of currents and the convective (parallel) electron heat transport. The differential operator definitions are

$$\nabla_\parallel = 1/(g)^{1/2}\ \partial/\partial\xi\ (h_\xi h_\psi), \qquad \underline{\nabla}_\parallel = 1/h_\xi\ \partial/\partial\xi\ ,$$

$$\nabla_\psi = 1/(g)^{1/2}\ \partial/\partial_\psi\ (h_\xi h_\zeta), \quad \text{and} \quad \underline{\nabla}_\psi = 1/h_\psi\ \partial/\partial\psi\ ,$$

where h_ξ, h_ζ, h_ψ, and $(g)^{1/2} = h_\xi h_\zeta h_\psi$ are the metric coefficients. In deriving the equations, the terms in the divergence operator containing the drift velocity v_ζ and the derivative $\partial/\partial\zeta$ have been replaced by the terms containing $\partial/\partial\xi$, $v_\parallel \equiv v_\xi$, and v_θ. To accomplish this, the geometric relationships $1/h_\zeta\ \partial/\partial\zeta = (B_\phi/B_\theta)/h_\xi\ \partial/\partial\xi$ and

$$v_\parallel = v_\theta \frac{B}{B_\theta} - v_\zeta \frac{B_\phi}{B_\theta}\ , \tag{5}$$

have been used. Here v_ζ is the drift velocity within the poloidal flux surface in the $\nabla\psi \times \underline{B}$ direction. It is seen that without ion drifts ($v_\zeta = 0$)

$v_\parallel = v_\theta B/B_\theta$, and the Eqs. (1)-(4) take on the familiar form. Inspection of Eq. (1) shows that $nv_\theta(B/B_\theta)$ can be regarded as an effective parallel flux, with the same conservation properties as $nv_\parallel$ in the absence of drifts. The radial velocity is both diffusive and convective,

$$v_\psi = (\nabla_\psi n)/n + (c/e)F_\zeta/B, \quad \text{and} \quad v_\zeta = (c/e)\, F_\psi/B\ ,$$

$$\text{with} \quad \underset{\sim}{F} = -e\underset{\sim}{\nabla}\Phi - (\underset{\sim}{\nabla} p)/n. \tag{6}$$

All the radial transport coefficients are empirical, and Spitzer conductivity is used for parallel transport. Since the magnitude of the force $\underset{\sim}{F}$, used to compute drifts by $\underset{\sim}{v}_d = (c/e)\ (\underset{\sim}{F} \times \underset{\sim}{B})/B^2$, is typically 100 electron volts/cm in large tokamaks, the inertial forces due to curvature, being two orders of magnitude smaller, have been neglected. For electrons, the radial force balance is approximately zero (because of $e\Phi \approx T$), so they are roughly stationary outside the recycling region. Only classical viscosity has been considered since there is no applicable neoclassical theory and no relevant experimental data. The parallel friction force has been neglected in Eq. (3) though it could produce a potential change of ~0.1 T over the full field line length.

The equations (1)-(4) have been solved numerically in D-III-D scrape-off geometry, shown in Fig. 2 together with temperature contours. A power flux of 2 MW across the separatrix was assumed together with zero particle flux, $\partial v_\parallel/\partial\psi = 0$, and a constant potential on the main plasma boundary. With these conditions it has not been necessary to specify either n, T , or $\underset{\sim}{v}$ on this boundary. The most dramatic feature of the results is the steep increase in pressure and the corresponding increase in the electrostatic potencial on the

field lines which pass close to the X-point. This phenomenon is due to the fact that there is a ridge in the potential and pressure surfaces in the region between the X-point and the plate. As a consequence, the ψ component of $\underline{F}$ in Eq. (6) changes direction on the ridge and results in $F_\psi = 0$ and $v_\parallel = 0$, according to (5), along a line close to the ridge which nearly coincides with the portion of separatrix between the X-point and the plate. Therefore, both $v_\parallel$ and v_ϕ (v toroidal) change sign on this line, while v_ψ has a maximum there. This assumes $v_\theta\ (B/B_\theta) \ll v_s$ in Eq. (5). This is true just below the X-point in Fig. 2, because the equipotentials, and, therefore, the drift surfaces, are near-orthogonal to the magnetic flux surfaces there resulting in negligible poloidal drifts. (The equipotentials resemble the closed magnetic flux surfaces even outside the separatrix.) In general, the direction of $\underline{F}$ is such that a circulatory flow is produced outside the main plasma boundary unimpeded by the branching of the separatrix. The jump in pressure can be understood by inspecting Eq. (2). Both the poloidal (v_θ) and radial (v_ψ) motion brings the parallel momentum into the volume (ΔV) to the right of the separatrix and just below the X-point, indicated in Fig. 2. The plasma which exits from this volume across the separatrix, has zero parallel momentum, so there is a net influx of momentum into ΔV. To conserve momentum, $\underline{\nabla}_\parallel(2nT)$ must balance this influx according to Eq. (2). This explanation results from the Eulerian approach used in solving the equations. In the Lagrangean picture a fluid volume stays on a flux surface as long as the equipotential and flux surfaces coincide. Near the X-point the flux surfaces become near-orthogonal to the equipotentials and the parallel momentum drives the fluid up the potential. This destroys the parallel momentum and creates a pressure gradient. The ion fluid is then accelerated again in the opposite toroidal direction as it continues to drift clockwise below the X-point. The process is then repeated on the inner separatrix branch.

The pressure variations along a field line close to the separatrix for the case with and without drifts are shown in Fig. 3. The initial pressure rise near the plates is due to the change in $v_\parallel$ from $v_\parallel = v_s$ at the sheath to $v_\parallel = 0$ near the outer edge of the recycling region. Without drifts the pressure is nearly constant between the two recycling regions, while with drifts the pressure increases abruptly as the X-point is approached. The pressure gradient near the X-point is in our case limited by the mesh resolution, while in reality it must be limited by viscosity. We estimate that classical viscosity should become important for parallel scale lengths of 100 cm or less, assuming the present solution parameters.

The potential variation corresponding to the pressure jump according to Eq. (3) is shown in Fig. 4. The potential step near the X-point is close to $\Delta(e\Phi) \approx T$ in magnitude.

While the significance of the described results for the H-mode has not been proven, a number of features of the solution suggest that the potential steps near the X-point could trigger the H-mode. These steps are barriers for hot electrons and should reduce heat conduction in a manner similar to that suggested by Ohkawa et al.[12] This is supported by measurements on D-III-D[13] which show a 50% increase in T_e in the scrapeoff just before the transition while pressure stays constant, indicating no change in the heat flux across the separatrix. There are experimental indications that large poloidal forces, causing drifts in the direction of the major axis, must exist near the X-point. Only drifts in the region of weak B_θ, where poloidal gyro-radius is large, can explain the inward shifts in the power profiles observed on D-III-D[14] and ASDEX.[15] On D-III, the toroidal field was in the opposite direction (∇B drift away from X-point), and the power profile was shifted outward,[16] in agreement with our model. Correspondingly, the

profile which is shifted towards the separatrix is compressed, while the other profile is expanded. The same is observed on JFT2M[17] together with a change in the outer to inner parallel power flux ratio, which can be related to the clock-wise versus anti-clockwise convection.

The size of the potential step is temperature and power dependent. (Across the step one can expect a $P \sim T^{3/2}$ rather than a $P \sim T^{7/2}$ power-temperature relationship.) From Eqs. (2), (3), (5), and (6), we find approximately for the potential step

$$\Delta(e\Phi) \sim mv_{\parallel}v_{\theta}B/B_{\theta} \sim mv_{\parallel}^2 \sim m(\nabla_{\psi}T/B_{\theta})^2 \sim mT^2/(\lambda_{\psi}B_{\theta})^2.$$

Assuming that $\Delta(e\Phi)/T$ is a constant for all transitions, we get the following scaling for the transition temperature on the separatrix: $T_{tr} \sim (\lambda_{\psi}B_{\theta})^2/m$, where λ_{ψ} is the radial (midplane) temperature scale length.

The smaller the λ_{ψ}, the lower the threshold. Assuming it is the outer scrapeoff λ_{ψ} that matters, lower thresholds can be expected when the $\nabla\underline{B}$ drift is towards the X-point. In this case the $\underline{E} \times \underline{B}$ drifts act against diffusion outside the separatrix narrowing the outer temperature profile, while inside the drifts and diffusion are in the same direction, widening the profile.

Inspection of Eq. (2) shows that the solution would bifurcate at $v_{\theta} = 0$, for a constant temperature ($\partial T/\partial \xi = 0$). However, under realistic conditions, it seems that only one solution branch is possible. In the case of the ∇B drift towards X-point, it is the branch which gives clockwise poloidal flow around the main plasma. Apart from their possible relevance for the H-mode, the new hydrogen flow solutions have important consequences for the impurity transport. For instance, while for hydrogen poloidal drifts just dominate over parallel motion for moderately high Z impurity, the hydrogen drag would

dominate poloidal drifts, and impurities would travel poloidally in the opposite direction from hydrogen. It is seen that the consequences of the ion drifts are very numerous and could be far reaching. However, a better knowledge of the transport coefficients, viscosity in particular, and the effect of potential barriers is required before a quantitatively accurate scrape-off plasma model can be constructed.

ACKNOWLEDGMENT

This work was supported by the U.S. Department of Energy Contract No. DE-AC02-76-CHO-3073.

REFERENCES

[1]B.J. Braams, Europhysics Conference Abstracts, 7D-II, 431 (1983).

[2]U.L. Igitkhanov et al., Europhysics Conference Abstracts, 7D-II, 397 (1983).

[3]S. Saito et al., J. Nucl. Mater. 121, 199 (1984).

[4]M. Petravic et al., J. Nucl. Mater. 128&129, 111 (1984).

[5]B.J. Braams, NET Report No. 68, January 1987.

[6]N. Ueda et al., Report JAERI-M 87-119, July 1987.

[7]S.I. Braginskii, Reviews of Plasma Physics, Vol. I (Consultants Bureau, NY, 1965) p. 205.

[8]M. Petravic et al., Phys. Rev. Lett. 48, 326 (1982).

[9]M. Petravic et al., J. Nucl. Mater. 128&129, 91 (1984).

[10]F. Wagner et al., Phys. Rev. Lett. 49, 1408 (1982).

[11]C.E. Singer and W.D. Langer, Phys. Rev. A 28, 994 (1983).

[12]T. Ohkawa et al., Phys. Rev. Lett. 51, 2101 (1983).

[13]K.H. Burrell et al., H-Mode Workshop, San Diego, CA, November 1987.

[14]D.N. Hill et al., IAEA Workshop on Hydrogen Retention, Princeton, NJ, July 1987.

[15]J. Neuhauser et al., H-Mode Workshop, San Diego, CA, November 1987.

[16]S. Sengoku et al., Nucl. Fusion 24, 415 (1984).

[17]N. Ueda, ITER Workshop on Impurity Control, Garching, FRG, May 1988.

FIGURE CAPTIONS

FIG. 1 The (ϕ,θ) and (ξ,ζ) coordinate systems, where ϕ is the toroidal and θ the poloidal angle. All the vectors lie within a poloidal flux surface.

FIG. 2 The basic geometry of the D-III-D tokamak. A poloidal plane is shown with the separatrix, vacuum walls, and temperature contours. ΔV is a small volume used in the discussion of the solution.

FIG. 3 Pressure variation along a field line close to the separatrix for the cases with and without ion drifts. The labels indicate plate (p), X-point (X), mid-plane (m), and top (t). The inner plate is on the left, and the outer plate is on the right.

FIG. 4 The electrostatic potential just outside the separatrix (1 mm in mid-plane), corresponding to the pressure solution with drifts of Fig. 3. The meaning of the labels is the same in the two figures.

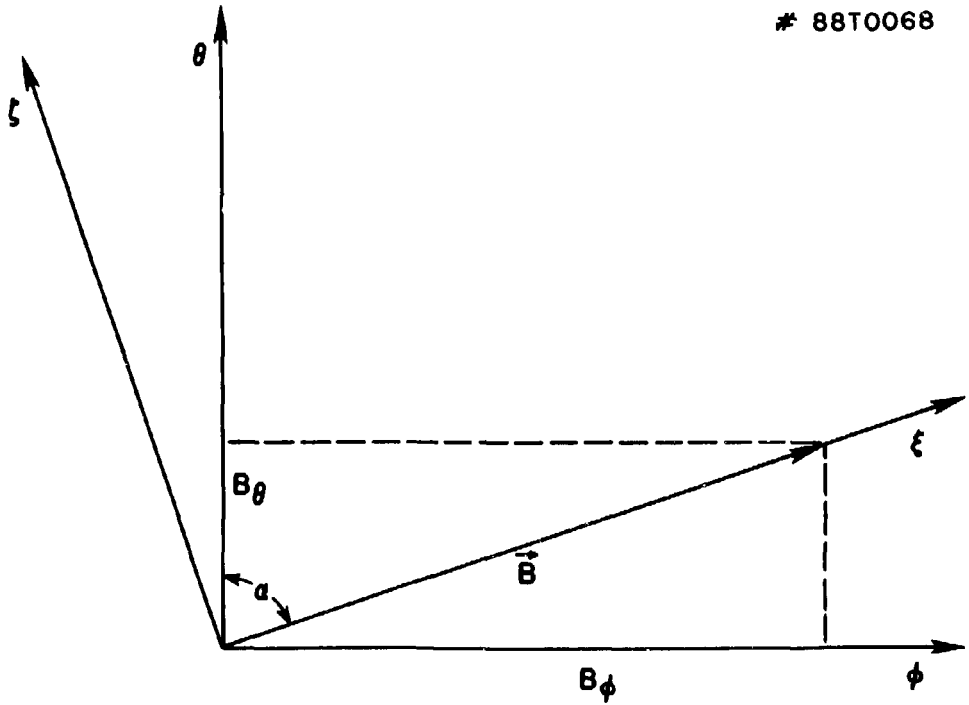

Fig. 1

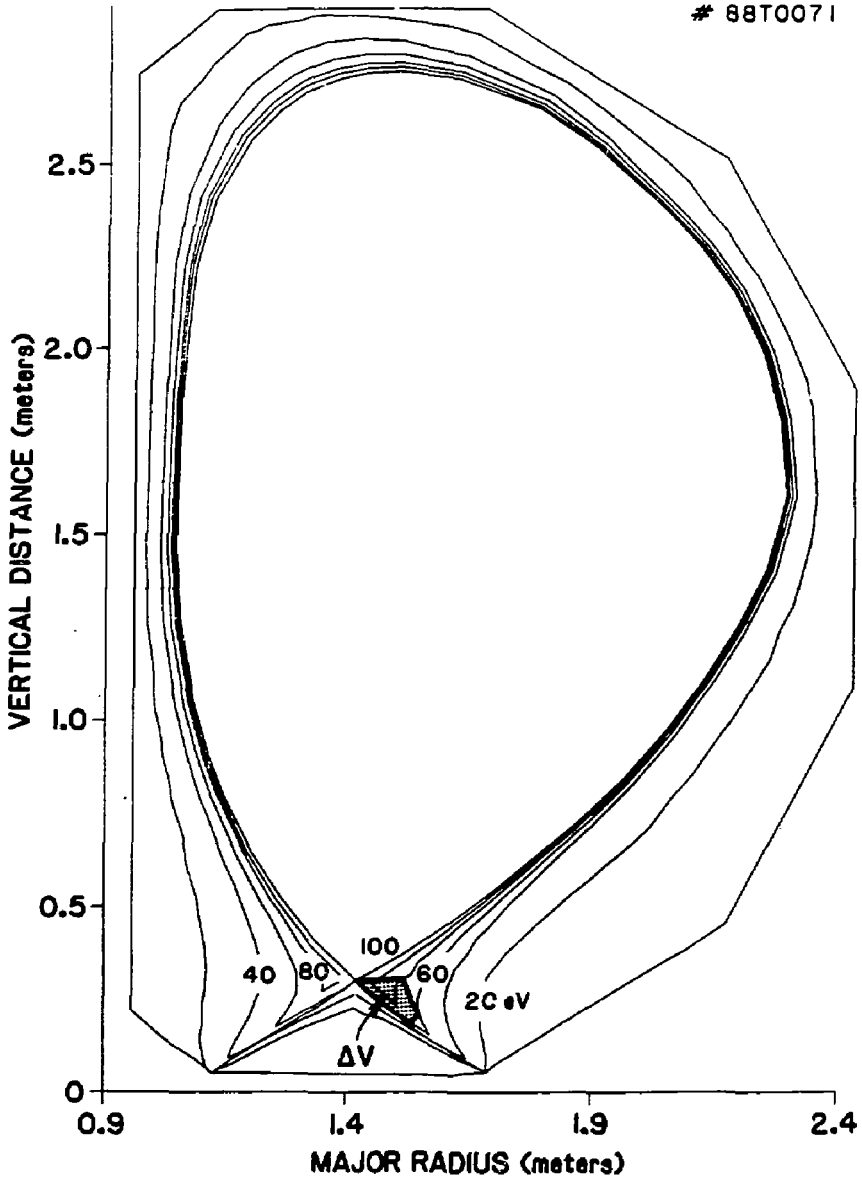
88T0071
2.5
2.0
1.5
1.0
0.5
0
VERTICAL DISTANCE (meters)
0.9
1.4
1.9
2.4
MAJOR RADIUS (meters)
100
40
80
60
20 eV
ΔV

Fig. 2

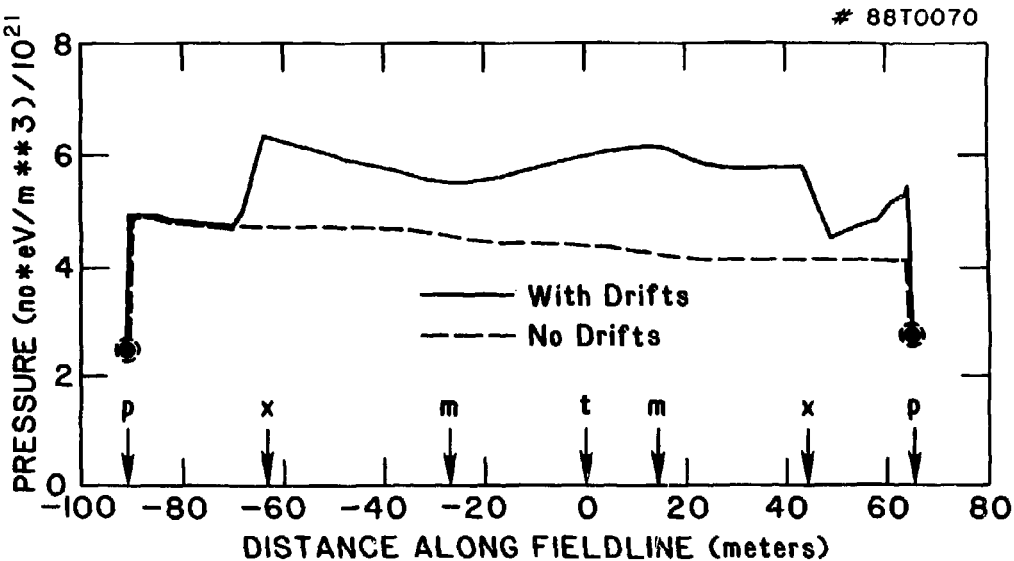
88T0070
PRESSURE (no*eV/m**3)/10^21
8
6
4
2
0
With Drifts
No Drifts
p
x
m
t
m
x
p
−100
−80
−60
−40
−20
0
20
40
60
80
DISTANCE ALONG FIELDLINE (meters)

Fig. 3

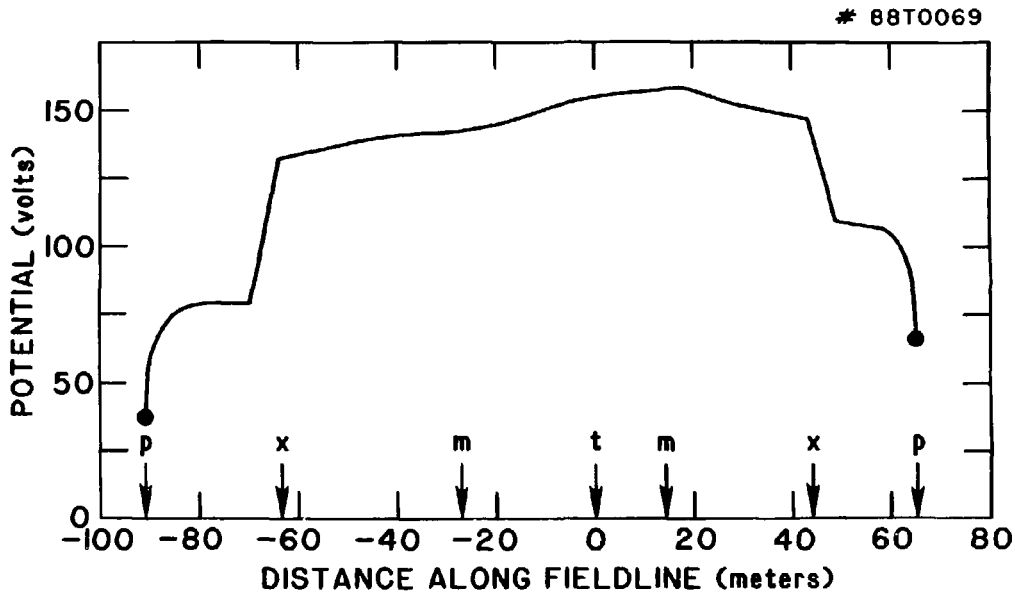
88T0069
POTENTIAL (volts)
150
100
50
0
p
x
m
t
m
x
p
-100
-80
-60
-40
-20
0
20
40
60
80
DISTANCE ALONG FIELDLINE (meters)

Fig. 4